iScience

Article

Analysis of chromatin accessibility associated with azacitidine response in higher-risk myelodysplastic neoplasms

Graphical abstract

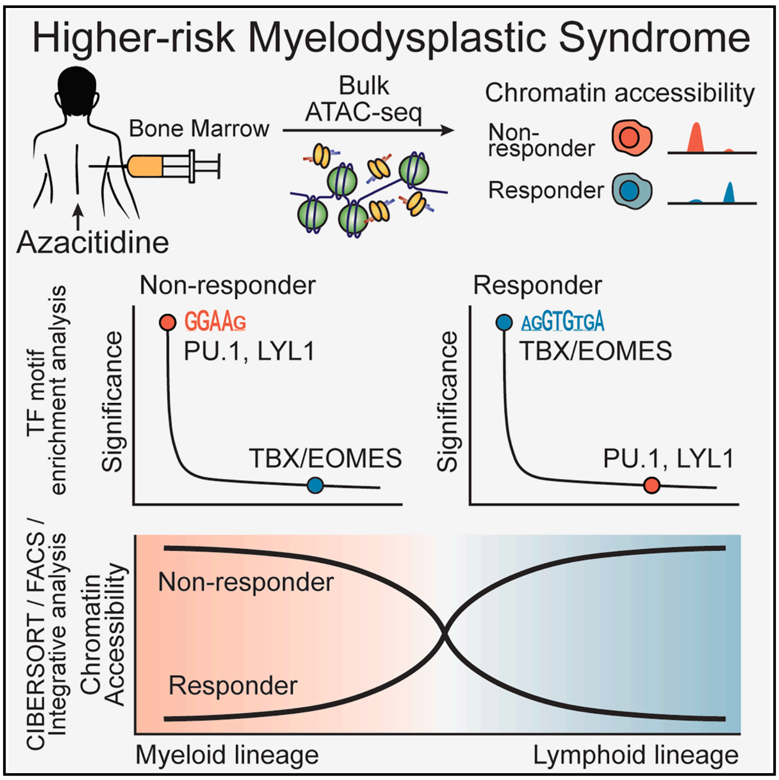

Highlights

- ATAC-seq reveals distinct accessible genome associated with AZA responses in HR-MDS
- Non-responders show enrichment of regulatory elements linked to myeloid progenitor programs
- TBX/EOMES motifs are highly opened in responders, reflecting differentiated CD8$^+$ T cells
- Bone marrow of non-responders contains reduced cytotoxic T cell populations

Authors

Dayoung Kim, Silvia Park, Yong-Rim Kwon, ..., Hee-Je Kim, Yoo-Jin Kim, Seung Woo Cho

Correspondence

cumckim@catholic.ac.kr (H.-J.K.),
yoojink@catholic.ac.kr (Y.-J.K.),
swcho@unist.ac.kr (S.W.C.)

In brief

Health sciences; Internal medicine; Medical specialty; Medicine; Oncology

Kim et al., 2025, iScience 28, 113297
September 19, 2025
https://doi.org/10.1016/j.isci.2025.113297

CellPress

CellPress OPEN ACCESS

Article

Analysis of chromatin accessibility associated with azacitidine response in higher-risk myelodysplastic neoplasms

Dayoung Kim,[1,8] Silvia Park,[2,8] Yong-Rim Kwon,[2] Heejei Yoon,[2] Byung-Sik Cho,[2] Inwha Baek,[3] Joo H. Kang,[1] Tae-Eun Park,[1] M. Ryan Corces,[4,5,6] Hee-Je Kim,[2,*] Yoo-Jin Kim,[2,*] and Seung Woo Cho[1,7,9,*]

[1]Department of Biomedical Engineering, College of Information and Biotechnology, Ulsan National Institute of Science and Technology, Ulsan 44919, Korea

[2]Department of Hematology, Catholic Hematology Hospital, Seoul St. Mary's Hospital, College of Medicine, The Catholic University of Korea, Seoul 06591, Korea

[3]College of Pharmacy, Kyung Hee University, Seoul 02447, Korea

[4]Gladstone Institute of Neurological Disease, San Francisco, CA 94158, USA

[5]Gladstone Institute of Data Science and Biotechnology, San Francisco, CA 94158, USA

[6]Department of Neurology, University of California, San Francisco, San Francisco, CA 94158, USA

[7]Center for Genomic Integrity, Institute for Basic Science, Ulsan 44919, Korea

[8]These authors contributed equally

[9]Lead contact

*Correspondence: cumckim@catholic.ac.kr (H.-J.K.), yoojink@catholic.ac.kr (Y.-J.K.), swcho@unist.ac.kr (S.W.C.)

https://doi.org/10.1016/j.isci.2025.113297

SUMMARY

Azacitidine, used in the treatment of higher-risk myelodysplastic neoplasms, is a DNA methyltransferase inhibitor that modifies epigenetic regulatory programs. The efficacy of azacitidine varies among patients, with approximately 50% of patients failing to respond. However, whether epigenomic factors affect responses to azacitidine has not been investigated. We examined chromatin accessibility in bone marrow cells from 23 treatment-naive patients with higher-risk myelodysplastic syndrome, suggesting azacitidine response is strongly associated with distinct hematopoietic cell states. Chromatin-accessible regions in non-responders were enriched for myeloid progenitor signatures, whereas those in responders were enriched for T cell signatures. Notably, $CD8^+$ T cells from non-responders exhibited reduced chromatin accessibility at TBX/EOMES-binding sites, bridging T cell differentiation state and azacitidine response. These findings suggest that immune cell function contributes to the responses to hypomethylating agents in myelodysplastic neoplasms and that chromatin accessibility could be used to predict drug responses in high-risk myelodysplastic syndrome patients.

INTRODUCTION

Azacitidine (AZA) is a pyrimidine nucleoside analog of cytidine that inhibits DNA methylation, resulting in changes in global gene expression and cell fate.[1,2] AZA is considered a standard treatment for patients with higher-risk myelodysplastic neoplasms (HR-MDS), particularly in elderly patients who are ineligible for intensive chemotherapy or allogeneic hematopoietic stem cell (HSC) transplantation.[1,3,4] Nevertheless, only about half of HR-MDS patients achieve responses to AZA,[5,6] and these are ultimately lost in most cases.[7,8] Furthermore, AZA treatment failure, whether primary or secondary, results in a dismal prognosis and often leads to progression into secondary acute myeloid leukemia (AML).[7,8] In light of these clinical challenges, predictive biomarkers for AZA sensitivity and resistance are needed to optimize therapeutic strategies. Previous studies have explored genetic mutations, DNA methylation, and gene expression as potential predictors of AZA response.[9–13] However, the clinical relevance of these factors has been challenging to translate from genomics to patient treatment.[14–17]

Chromatin accessibility is a critical feature determining the activity of gene regulatory elements, such as enhancers and transcription factor binding sites,[18,19] and is often inversely correlated with DNA methylation. Cell-type specific regulation of chromatin accessibility is crucial for the differentiation and function of various cell types and has been linked to disease progression and treatment responses in specific cell populations, such as $CD34^+$ hematopoietic stem and progenitor cells in AML.[20] Studies have also shown that changes in chromatin accessibility can precede alterations in gene expression.[20,21] Therefore, analyzing chromatin accessibility could effectively identify factors that influence drug responses.

Here, we demonstrate that chromatin states are significantly different between AZA responders and non-responders in

HR-MDS patients. Chromatin accessibility analysis revealed that non-responders exhibited high levels of myeloid cell signatures and displayed regulatory networks resembling those observed in primary AML. Additionally, the AZA response was related to lymphoid programs, specifically the activation of CD8$^+$ T cells function in responders. These findings identify important gene regulatory signatures involved in shaping AZA treatment outcomes and provide key insights into the treatment response.

RESULTS

To investigate chromatin accessibility profiles associated with AZA sensitivity and resistance in HR-MDS patients, we conducted the assay for transposase-accessible chromatin using sequencing (ATAC-seq) on fresh-frozen AZA naive bone marrow samples from 23 patients. (Figure 1A; Table 1). Among these patients, 15 were responders (MDS-R) to AZA treatment, while 8 were non-responders (MDS-NR) (See method details). Also, to provide broader context and comparative analysis, we generated ATAC-seq data from healthy bone marrow controls (n = 3) and primary AML patient samples (n = 13) (Table S1).

Unsupervised hierarchical clustering and principal component analysis revealed distinct chromatin accessibility signatures between azacitidine responders (MDS-R) and non-responders (MDS-NR), independent of clinical variables, such as age, sex, and international prognosis scoring system risk (Figures 1B, 1C, and S1A–S1D). The blast percentage in the response group did not differ from that in the non-response group (Figure S1E).

These distinct chromatin accessibility patterns also showed higher cluster purity than those of DNA methylation[13] and RNA-seq[12] datasets (Figures S1F and S1G). Differential accessibility analysis revealed that 1,940 peaks were associated with the AZA response (Figure 1D; Table S2), with only 7.1% located in exons and 24.6% in promoter-proximal regions (Figure S1H). The reliability of these differential peaks was confirmed by bootstrapping analysis (Figure S1I), ruling out unexpected artifacts. Overall, chromatin accessibility measured by ATAC-seq successfully revealed and distinguished epigenetic differences associated with the AZA response in MDS patients, suggesting that the regulatory functions of the non-coding genome may be pivotal in cancer drug responses.

Within gene regulatory networks, transcription factors (TFs) are key regulators of gene expression and cell fate determination of HSCs.[20,22] To analyze the functional implications of response-specific regulatory features, we performed TF motif enrichment analysis on promoter-distal peaks in the ATAC-seq data (Figure 1E).

For the MDS-NR peaks, we observed a significant enrichment of PU.1 family TF-binding motifs, SPI1/SPIB, which serve as master regulators of myeloid lineage commitment[23,24] and lymphoid suppression.[25,26] The MDS-NR peaks also showed enrichment for LYL/OLIG motifs, particularly LYL1, a TF overexpressed in AML.[27] To validate our transcription factor motif enrichment analysis, we compared MDS-NR peaks containing PU.1 or LYL1 motifs with chromatin immunoprecipitation sequencing (ChIP-seq) binding data from healthy hematopoietic progenitors[28] (Figure S2A). PU.1 motifs from MDS-NR peaks, showed actual PU.1 binding in healthy CMP cells, representing a 3.76-fold enrichment (false discovery rate [FDR] = 3.58×10^{-99}) over background. Similarly, MDS-NR peaks with LYL1 motifs were validated by actual LYL1 binding in healthy GMP cells, showing 3.63-fold enrichment (FDR = 1.06×10^{-42}) over background (Figure S2A). These results support our findings, suggesting that the regulatory elements accessible in MDS non-responders are indeed bound by PU.1 and LYL1 in relevant myeloid progenitor populations.

These findings led us to compare the chromatin accessibility profiles of HR-MDS with those of primary AML. Integrative analysis revealed that the chromatin accessibility patterns of AML patients closely resembled those of MDS-NR patients (Figures 1C and S2B; Table S3). Notably, 61 out of 171 shared peaks between MDS-NR and AML contained SPIB/SPI motifs (FDR = 7.78×10^{-5}), suggesting that AZA non-responders in HR-MDS and AML patients may share similar regulatory states (Figure 1F).

Next, we found that four out of 132 protein-coding genes adjacent to the MDS-NR peaks, which were upregulated AZA-associated genes in the Comparative Toxicogenomic Database (Table S4; Figure S2C). Among these, *ST3GAL6* overexpression is linked to poor survival in multiple myeloma,[29] while *RUNX1*, which cooperates with PU.1, plays an essential role in HSC differentiation and leukemia development.[30] Indeed, *ST3GAL6*, *RUNX1*, and *PROM1* showed high expression level in primitive HSCs, leukemic stem cells, and blast cells, compared to the differentiated blood cell populations,[31] supporting its association with stemness and undifferentiated cellular states.[32,33] Indeed, gene set enrichment analysis revealed enhanced ATAC-seq accessibility at HSC-associated genes in MDS-NR patients (Figure S2D), consistent with previous studies linking HSC populations with treatment resistance to AZA.[34]

Conversely, the peaks that were specifically observed in AZA responders showed a distinct signature, marked by the motif enrichment of immune-regulatory TFs, identified through TF motif enrichment and gene set enrichment analysis. Notably, we observed a frequent enrichment of FOX family genes and motifs (Figures 1E and S3A), which regulate T cell development and function, alongside TBX/EOMES-binding motifs (Figure 1E), which have crucial roles in the development of cytotoxic and memory T cells[35] and the antitumoral activity in lymphoid leukemia.[36] The biological significance of these immune-associated features was further supported by the upregulation of immune response genes in responders (Figure S3B). Specifically, the interferon-gamma encoding gene *IFNG*, a key cytokine involved in anti-tumor immunity and immune surveillance, was upregulated in MDS-R patients[12] (Figure S3C). Taken together, the chromatin accessibility landscape revealed potential differences in regulatory programs between non-responders and responders prior to AZA treatment: non-responders exhibited potential activation of genes and regulatory programs associated with AML and HSC, while responders showed enrichment of immune pathways suggesting heightened activity of the immune response in MDS-R. These findings suggest that pre-existing differences in hematopoietic cell lineage composition may contribute to variability in response to AZA treatment in MDS patients.

Bone marrow cells are composed of various cell types that differentiate from HSCs. We speculated that the distinct differences we observed between MDS-R and MDS-NR patients

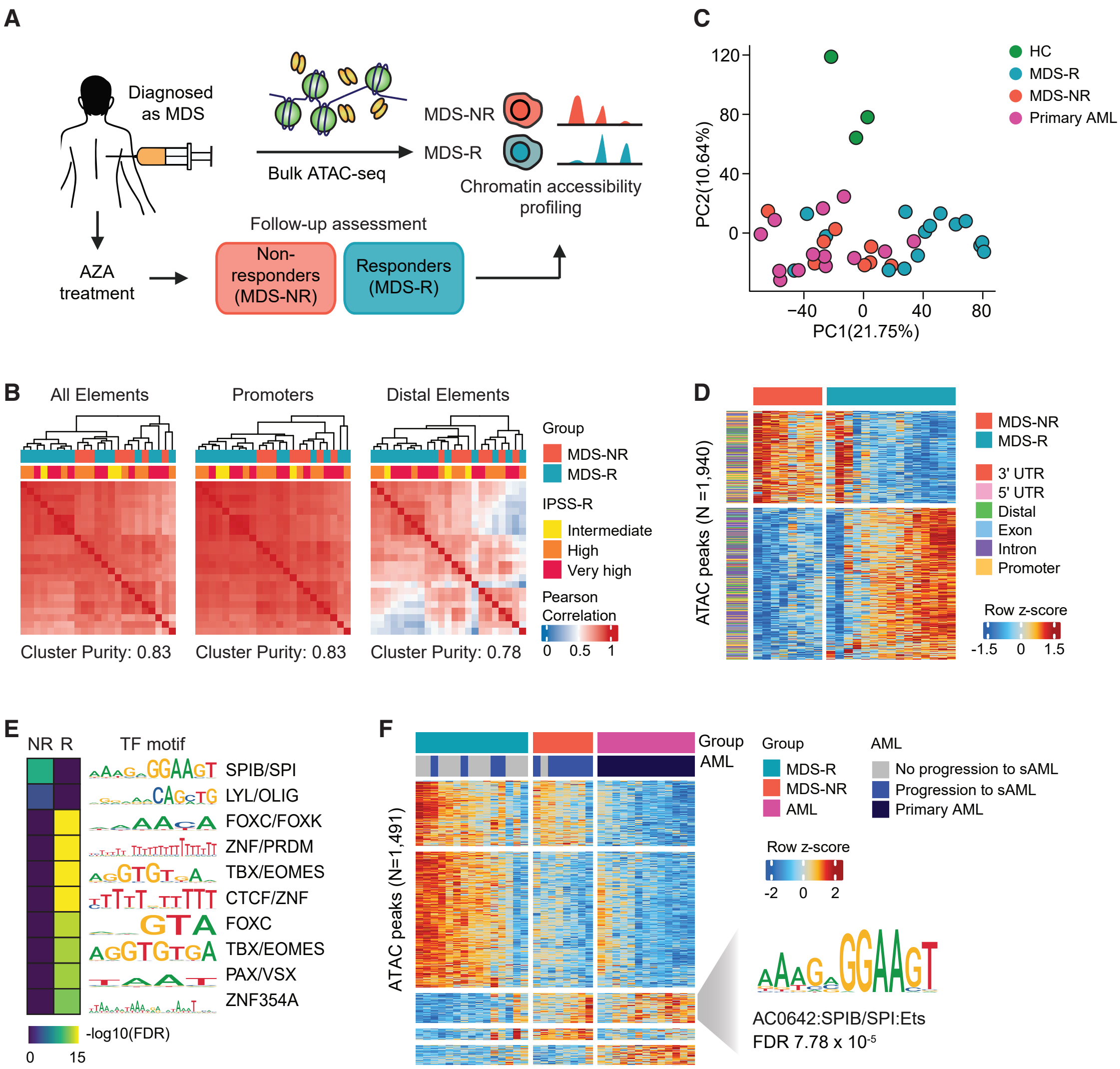

Figure 1. Genome-wide chromatin accessibility profiling reveals distinct patterns in HR-MDS associated with AZA responses

(A) Schematic overview of bulk ATAC-seq using cryopreserved, unfractionated bone marrow mononuclear cells from AZA-naïve HR-MDS patients.

(B) Pearson correlation analysis across patients using all peaks (n = 32,718), promoter peaks (peaks within -1 kb to +100 bp from the transcription start site (TSS, n = 16,789), and distal elements (all but promoter peaks, n = 15,929). Cluster purity scores are written under the heatmaps. The revised international prognostic scoring system (IPSS-R) is divided into three groups based on risk; intermediate (3.5–4.5), high (5.0–6.0), and very high (greater than or equal to 6.5).

(C) Principal-component analysis of all regulatory elements distinguishing 8 MDS-NR, 15 MDS-R patients, three healthy controls (HC), and 13 primary AML patients.

(D) Heatmap of differentially accessible regions between MDS-NR and MDS-R groups ($p < 0.05$, $|FC|>1.5$), including both promoter-proximal and distal regions. The left annotation shows the genomic features mapped to the left of the heatmap.

(E) TF motif enrichment analysis in differential distal elements (MDS-NR peaks and MDS-R peaks), displayed as a heatmap showing -log10 of adjusted hypergeometric p values (Benjamini-Hochberg correction). The corresponding binding motifs are in the middle panel, alongside their representative TFs (right).

(F) Heatmap of the results of differential accessibility analysis of MDS and primary AML patients ($p < 0.05$, $|FC|>1.5$). Whether MDS patients progressed to secondary AML (sAML) or not is shown in the second row of color bars. The ATAC-seq peaks that were common to MDS-NR and AML patients are shown at the third block of peaks row-wise, and the enriched transcriptional factor motif is shown at the right. FDR is the adjusted hypergeometric p value as described in (E).

See also Figures S1–S3.

could be due to differences in the cellular composition of bone marrow between these patients. Hematopoietic cell-type proportions were inferred through computational deconvolution of bulk ATAC-seq data using CIBERSORTx[37] (Figure 2A; Table S5, See method details), revealing that bone marrow from MDS-NR patients was enriched in progenitor cells, especially common myeloid progenitors (CMPs) and granulocyte-macrophage progenitors (GMPs), while bone marrow from MDS-R patients was enriched in lymphoid cells, particularly $CD8^+$ T cells (Figure 2B). Indeed, the chromatin accessibility of MDS-NR and MDS-R peaks across different hematopoietic cell populations[20] also demonstrated their contrasting cell-type specific

Table 1. Clinicopathologic characteristics of patients with myelodysplastic syndrome

GEO ID	Sex/ Age	WHO 2016	BM Blast (%)	Cytogenetics	Mutations	Response	Total cycles	Subsequent	Survival (duration, months)
MDS_01	M/75	MDS-EB-2	17	45,XY,add(1)(p13),der(3) add(3)(p13)add(3)(q11.2), der(5)t(1; 5)(p22; q22), der(7; 17)(p10; q10),add(17) (q25),-21,+mar [cp10]/50, idem,der(3),+3,+der(5)t(1; 5), der(7; 17),+8,+11,+13,+14, 17,+21[cp8]/46,XY[2]	*TP53*	SD + HI	4	No	dead (3.9)
MDS_02	M/62	MDS-EB-2	18	46,XY[20]	*DNMT3A*, *SF3B1*, *RUNX1*, *BCOR*	1 failure with PD	4	Yes	dead (9.3)
MDS_03	M/73	MDS-EB-2	9	47,XY,+21[6]/46,XY[14]	*ASXL1*, *CREBBP*, *RUNX1*, *STAG2*	1 failure with PD	2	No	dead (7.6)
MDS_04	M/66	MDS-EB-2	14	46,XY[20]	*ASXL1*, *ETNK1*	MCR+HI	5	Yes	alive (41.5)
MDS_05	M/70	MDS-EB-1	9	46,XY,del(1)(p34.1p36.1) [16]/46,XY[4]	*TET2*, *ASXL1*, *SRSF2*, *TET2*	1 failure with PD	2	No	dead (16.3)
MDS_06	M/71	MDS-EB-1	8	46,XY[20]	NA	MCR+HI	5	No	dead (31.0)
MDS_07	F/71	MDS-EB-1	8	46,XY[20]	NA	MCR-HI	5	No	dead (23.0)
MDS_08	M/69	MDS-EB-1	7	46,XY[20]	NA	1 failure with PD	4	No	dead (33.8)
MDS_09	M/53	MDS-EB-2	17	47,XY,+8[18]/46,XY[2]	*DNMT3A*, *RUNX1*, *SRSF2*	SD + HI	5	Yes	alive (41.0)
MDS_10	M/66	MDS-EB-2	16	46,XY[20]	*STAG2*, *ASXL1*, *SRSF2*, *RUNX1*	1 failure with PD	1	Yes	dead (11.0)
MDS_11	M/58	MDS-EB-2	11	46,XY[20]	Not detected	1 failure with SD	4	Yes	dead (35.5)
MDS_12	M/60	MDS-EB-1	8	46,XY[20]	NA	MCR-HI	10	Yes	dead (119.9)
MDS_13	M/69	MDS-EB-2	10	47,XY,+8[19]/46,XY[1]	*ASXL1*, *EZH2*, *RUNX1*, *TET2*, *TET2*, *ZRSR2*	SD + HI	4	No	dead (5.9)
MDS_14	M/42	MDS-EB-2	10	46,XY[20]	NA	1 failure with PD	4	Yes	alive (104.3)
MDS_15	M/61	MDS-EB-1	5	46,XY[20]	NA	SD + HI	4	Yes	alive (157.2)
MDS_16	M/72	MDS-EB-2	12	46,XY[50]	NA	1 failure with PD	2	No	dead (11.0)
MDS_17	M/60	MDS-EB-2	17	46,XY[20]	*DDX41*, *DDX41*	SD + HI	5	Yes	alive (58.3)
MDS_18	F/57	MDS-EB-2	15	46,XX,inv(9) (p12q13)[20]	*SF3B1*	MCR-HI	3	Yes	dead (4.0)
MDS_19	M/67	MDS-EB-2	16	46,XY[8]	*DNMT3A*, *U2AF1*, *MPL*, *CD101*	MCR-HI	7	No	dead (10.9)
MDS_20	M/57	MDS-EB-2	13	47,XY,+del(1)(p31), del(20)(q11)[20]	NA	SD + HI	4	Yes	alive (118.1)
MDS_21	M/61	MDS-EB-2	15	46,XY[20]	*DNMT3A*, *TET2*, *SF3B1*	CR	8	Yes	alive (70.8)
MDS_22	F/27	RCMD	4	46,XX[20]	NA	CR	10	Yes	alive (145.9)
MDS_23	M/68	MDS-EB-2	17	46,XY[20]	NA	CR	9	Yes	alive (116.2)

WHO, World Health Organization; MDS-EB, myelodysplastic syndrome with excess blasts, RCMD, refractory cytopenia with multilineage dysplasia; BM, bone marrow; CR, complete remission; MCR + HI, marrow complete remission with hematologic improvement; MCR-HI, marrow complete remission without hematologic improvement; SD + HI, stable disease with hematologic improvement; 1 failure, primary failure; PD, progressive disease; NA, not assessable.

regulatory signatures; MDS-NR peaks were highly accessible in HSC and progenitor cell types (Figure S4A), whereas MDS-R peaks exhibited increased accessibility in lymphoid populations, such as CD4^{+}, CD8^{+}, and natural killer (NK) cells (Figure S4B). To validate these findings, we randomly selected four MDS-NR and four MDS-R samples from our MDS cohort and determined cell-type composition in the samples without bias using CIBERSORTx and flow cytometry on bone marrow samples. As expected, we observed a moderate positive correlation of cell population measurements between flow cytometry and CIBERSORTx (R = 0.47, p = 0.02) (Figures S4C–S4F). However, the number of CD34^{+}, CD4^{+}, and CD8^{+} cells was not significantly different between the two groups, although the number of CD8^{+} cells tended to be higher in MDS-R samples (Figure S4G). While

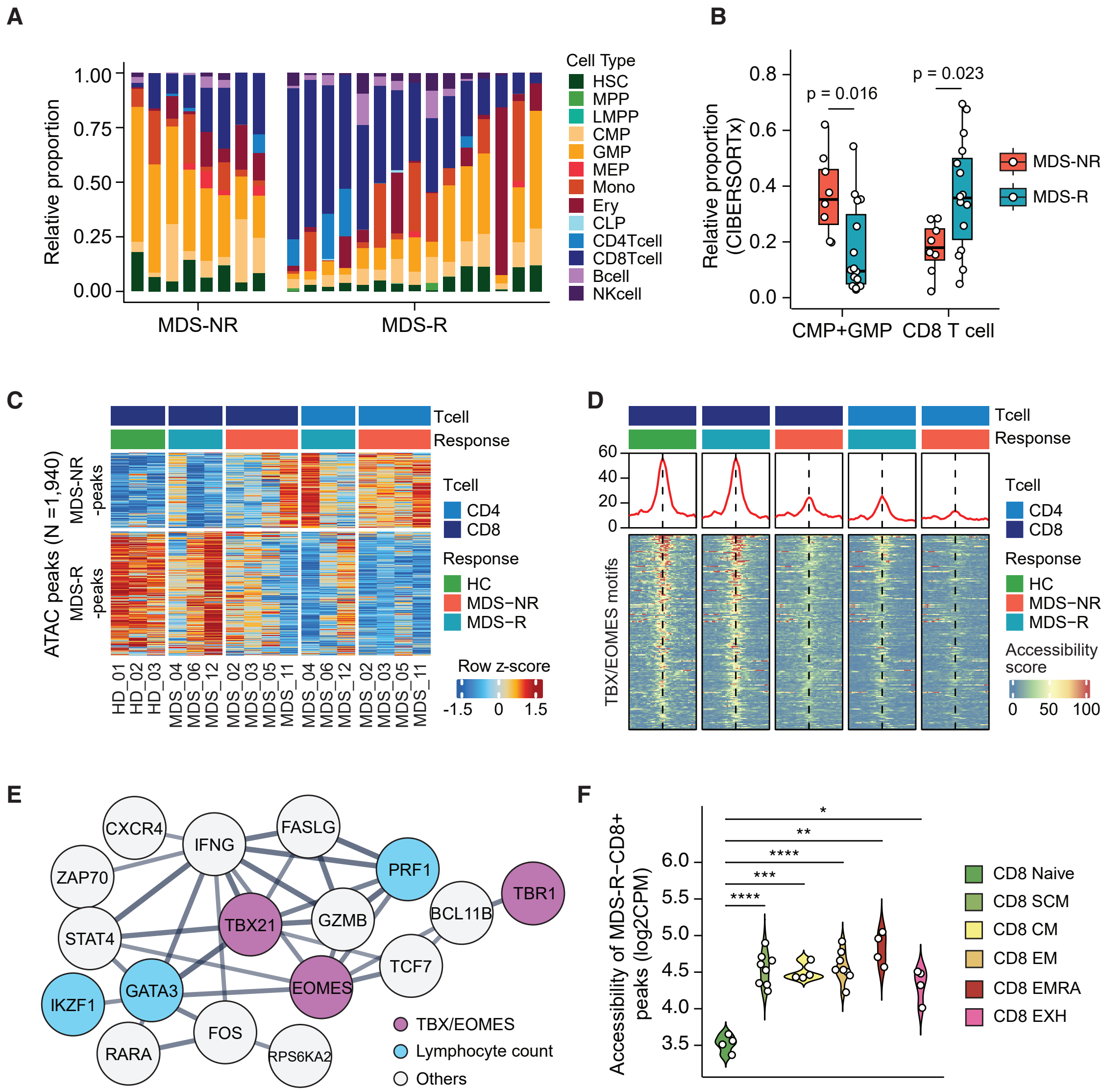

Figure 2. Cell type deconvolution of bone marrow correlating with AZA responses

(A) Hematopoietic lineage composition in MDS-NR and MDS-R patients determined by CIBERSORTx cell-type deconvolution using ATAC-seq data from normal human hematopoietic cells.[12] HSC, hematopoietic stem cell; MPP, multipotent progenitor; LMPP, lymphoid-primed multipotent progenitor; CMP, common myeloid progenitor; GMP, granulocyte-macrophage progenitor; MEP, megakaryocyte-erythroid progenitor; Mono, monocyte; Ery, erythroid; CLP, common lymphoid progenitor; CD4T cell, CD4$^+$ T cell; CD8T cell, CD8$^+$ T cell; Bcell, B cell; NKcell, natural killer cell.

(B) Boxplots display the abundance of CMPs and GMPs (CMP+GMP) and CD8$^+$ T cells in bone marrow samples, highlighting the significant difference between response groups. The boxplot displays the first quartile at the bottom, the third quartile at the top, and the median indicated by the thick line. Statistical differences were calculated by the Wilcoxon signed-rank test.

(C) Heatmap showing chromatin accessibility at differentially accessible regions between MDS-NR and MDS-R peaks identified in Figure 1D. Each column represents ATAC-seq data from CD4$^+$ or CD8$^+$ T cells isolated from MDS patient bone marrow samples. Individual patient IDs are indicated below.

(D) Aggregate plot of TBX/EOMES motif enrichment across different AZA response groups and T cell types. Upper panel: average accessibility profile centered on TBX/EOMES motifs present in MDS-R-specific peaks. Lower panel: heatmap showing mean accessibility scores across corresponding samples, with the motif center indicated by the dotted line and ±1 kb flanking regions.

(E) STRING[38] protein association network showing connections between genes near MDS-R-CD8$^+$ peaks which are uniquely accessible in CD8$^+$ T cells of MDS-R patients and TBX/EOMES transcription factors identified through motif analysis. Node colors indicate whether proteins are MDS-R-CD8$^+$ peak-associated genes or transcription factors from motif analysis. Edge thickness represents interaction confidence based on multiple evidence sources. Only proteins with two or more interactions of high confidence (interaction score $\geq$0.700) are shown.

(F) Chromatin accessibility of the MDS-R-CD8$^+$ peaks across human CD8$^+$ T cell differentiation subsets defined as naive population (naive), stem cell memory (SCM), central memory (CM), effector memory (EM), RA + effector memory (EMRA), and exhausted T cell (EXH) populations.[39] Each dot represents individual CD8$^+$ T cells, with peak scores calculated as the mean accessibility of the MDS-R-CD8$^+$. Statistical significance was determined using the Wilcoxon signed-rank test (*$p < 0.05$, **$p < 0.01$, ***$p < 0.001$, and ****$p < 0.0001$).

See also Figures S4 and S5.

differences in CD8+ T cell abundance likely contribute to the chromatin accessibility variation, our findings also indicate that qualitative differences in their functional states may play a substantial role in shaping the distinct epigenetic landscape associated with AZA response.

To further explore the basis of these distinct chromatin signatures, we conducted additional ATAC-seq on sorted CD8+ T cells from MDS bone marrow to analyze CD8+ T cell specific cells for chromatin alterations that might determine the AZA response, because frequent T cell dysfunction is observed in HR-MDS.[40,41] We observed that MDS-R peaks were highly accessible in CD8+ T cells from healthy controls and responders but were markedly reduced or inaccessible in CD8+ T cells from non-responders, suggesting that these regulatory regions are retained in MDS-R but specifically lost in MDS-NR patients (Figure 2C). These epigenetic changes were specific to CD8+ T cells, as they were not observed in CD4+ T cells, which generally share similar chromatin accessibility profiles with CD8+ T cells. Indeed, CD8+ T cells of responders and healthy controls—but not from non-responders—exhibited significant enrichment of TBX/EOMES-binding motifs (AC0489[42]), indicating that TBX21- and EOMES-regulated pathways in CD8+ T cells may play a critical role in shaping the AZA response (Figure 2D), consisting with our observations in bulk ATAC-seq analyses.

To further understand the molecular mechanisms underlying these differences between AZA response group in CD8+ T cells, we performed an integrative analysis of the ATAC-seq data of bulk and sorted T cells, focusing on MDS-R-CD8+ peaks that are uniquely accessible in responders and healthy controls. Network analysis integrating TBX/EOMES TFs and genes adjacent to MDS-R-CD8+ peaks revealed a regulatory network centered on lymphocyte count regulation (Figure 2E), with elevated expression of these genes in MDS-R patients[12] (Figure S5A). Intriguingly, this network included key cytotoxic T cell effector molecules, namely cytotoxic granules (*GZMB* and *PRF1*)[43,44] and interferon-γ (*IFNG*), which was supported by transcriptome analysis from a previous study[12] (Figure S3C). EOMES and TBX21 are known to regulate the expression of these effector molecules,[35,45] which were further supported by their coordinated expression (Figures S5B–S5D).

Additionally, when projecting MDS-R-CD8+ peaks onto single-cell ATAC-seq data from human CD8+ T cell subsets,[39] we observed higher accessibility in differentiated states than in naive states, confirming the role of TBX/EOMES regulation in proper T cell differentiation toward effector cells or memory cells (Figure 2F). Importantly, these peaks showed a greater enrichment in effector or memory T cells than in exhausted T cells. Altogether, these findings suggest that cytotoxic T cell activation is positively correlated with the AZA response in MDS patients.

DISCUSSION

This study presents a comprehensive analysis of the chromatin accessibility features that could predispose HR-MDS patients to respond or not respond to AZA treatment. We identified the significant differences in ATAC-seq peaks between AZA responders and non-responders. Our data then revealed that lineage-associated signatures—particularly those involving CD8+ T cell regulatory programs—emerged as among the most biologically meaningful features distinguishing these groups.

Whereas non-responders exhibited increased chromatin accessibility at regulatory regions associated with myeloid lineage programs, responders showed greater accessibility at loci linked to lymphoid, particularly CD8+ T cell, regulatory elements. Strikingly, the accessibility of SPIB/SPI-binding motifs in AZA non-responders closely resembled that observed in primary AML patients, suggesting a potential continuum in epigenetic dysfunction across myeloid malignancies that may contribute to impaired immune cell development in the bone marrow.[25]

Consistent with these findings, deconvolution analysis of bulk bone marrow revealed a higher abundance of myeloid progenitors in non-responders and CD8+ T cells in responders, which was validated by flow cytometry. This was further supported by integrative analyses using transcriptome data from ethnically matched individuals[12] and epigenome data from a Caucasian cohort.[20]

In order to disentangle the effects of cell type composition from cell-intrinsic chromatin accessibility signatures, we performed ATAC-seq on sorted CD8+ T cells. The result validated responder-specific CD8+ T cell peaks, with enrichment of TBX/EOMES-binding motifs, were present in healthy controls but absent in non-responders. These peaks exhibited the highest accessibility in differentiated cytotoxic T cells, particularly in their effector and memory states. Additionally, our findings are supported by the recent single-cell RNA-seq data demonstrating that CD8+ T cell subsets are associated with AZA response in myeloid neoplasms,[46] highlighting the relevance of CD8+ T cell function as a determinant of AZA response. We expect that individualized epigenomic profiles, derived from in-depth analysis including single-cell ATAC-seq, will result in greater precision in AZA treatment for MDS patients.

Our findings demonstrate that the landscape of chromatin accessibility can distinguish AZA responsiveness in MDS, even in bulk bone marrow cells. Moreover, DNA hypomethylating agents, such as AZA and decitabine, can directly promote tumor infiltration by CD8+ T cells and suppress tumor growth via anti-tumor cytolytic activity.[47–49] Considering the immunomodulatory function of AZA in myeloid malignancies[40,50] and tumors,[51–53] it is plausible that a pre-existing activation state of cytotoxic immune cells contributes to enhance the anti-cancer efficacy of AZA treatment. Indeed, our findings are consistent with recent research showing that immune responses and inflammatory signaling are enhanced in responders' CD34+ cells after AZA treatment,[54] collectively suggesting that AZA responses are associated with immune activation in bone marrow cells.

Together, our study suggests that AZA responders retain functional cytotoxic T cell programs through specific chromatin accessibility patterns, which may contribute to their favorable response to AZA treatment. This study provides early evidence supporting the potential of chromatin accessibility profiling to guide clinical decision-making in AZA treatment for HR-MDS, which will be strengthened with further validation in independent large cohorts supported by higher-resolution sequencing techniques.

Limitations of the study

This study reveals pre-existing distinct regulatory patterns in HR-MDS patients that appear to correlate with their responses to AZA treatment, suggesting the importance of cell regulatory states in bone marrow for determining AZA treatment outcomes. The rarity of HR-MDS, combined with strict inclusion criteria (i.e., therapy-naive patients who completed $\geq$5 AZA cycles), limited the sample size and precluded the use of more refined assays. Future studies employing sorted hematopoietic populations via flow cytometry and multimodal approaches will provide deeper understanding about the regulatory networks governing treatment response. Also, our results demonstrated the importance of both CD8$^+$ T cell abundance and their functional state. Further experiments will be required to determine whether these factors are equally important for both treatment responses or if one of these factors hierarchically influence the other. Finally, while our study focused on bone marrow samples, hematopoietic cells are present in both blood and bone marrow. Future comparative studies between these two different tissues could reveal interesting insights into the systemic nature of immune regulation in MDS and how it determines responses to AZA treatment. Although further high-resolution and mechanistic studies are needed, our results provide early evidence that chromatin accessibility profiling could serve as a valuable modality to inform clinical decision-making in the context of AZA treatment.

RESOURCE AVAILABILITY

Lead contact

Further information and requests for resources should be directed to and will be fulfilled by the lead contact, Seung Woo Cho (swcho@unist.ac.kr).

Materials availability

This study did not generate new unique reagents.

Data and code availability

The processed data files, including raw and normalized count matrix of the ATAC-seq data generated in this study, are available in the GEO: GSE291718.

ACKNOWLEDGMENTS

We thank members of the Genome Engineering Laboratory and UNIST for helpful discussions and assistance. This work was supported by a National Research Foundation of Korea Grant funded by the Ministry of Science and ICT, South Korea (NRF-2022R1A2C2006746 [to Y.-J.K.], RS-2023-00213043 [to S.W.C.], RS-2024-00509412 [to S.W.C.], RS-2024-00399800 [to S.W.C.]), and the Ministry of Education, South Korea (RS-2023-00275823 [to D.K.]).

AUTHOR CONTRIBUTIONS

D.K., S.P., Y.-J.K., and S.W.C. conceived and designed the project. D.K. performed ATAC-seq and data analysis. D.K., H.Y., and Y.-R.K. performed flow cytometry analysis and cell sorting. S.P., B.-S.C., H.-J.K., and Y.-J.K. collected and organized the biopsies and clinical information. I.B., J.H.K., T.-E.P., and M.R.C. contributed to methodology and informatic analysis. D. K. and S.W.C. wrote the original draft of the manuscript. D.K., S.P., I.B., J.H. K., T.-E.P., M.R.C., H.-J.K., Y.-J.K., and S.W.C. reviewed the manuscript.

DECLARATION OF INTERESTS

The authors declare no competing interests.

STAR★METHODS

Detailed methods are provided in the online version of this paper and include the following:

- KEY RESOURCES TABLE
- EXPERIMENTAL MODEL AND STUDY PARTICIPANT DETAILS
  - Patient information: Sample acquisition and clinical course
- METHOD DETAILS
  - Sample preparation and cell isolation
  - Flow cytometry and cell sorting
  - ATAC-seq library preparation
  - Processing bulk ATAC-seq data for analysis
  - Unsupervised k-means clustering and cluster purity
  - Identification of AZA-response-related ATAC peaks
  - TF motif enrichment analysis
  - Cell composition analysis using CIBERSORTx
  - Comparison with CD8$^+$ T cell subsets
- QUANTIFICATION AND STATISTICAL ANALYSIS

SUPPLEMENTAL INFORMATION

Supplemental information can be found online at https://doi.org/10.1016/j.isci.2025.113297.

Received: April 15, 2025
Revised: July 4, 2025
Accepted: August 1, 2025
Published: August 6, 2025

REFERENCES

1. Keating, G.M. (2009). Azacitidine: a review of its use in higher-risk myelodysplastic syndromes/acute myeloid leukaemia. Drugs *69*, 2501–2518. https://doi.org/10.2165/11202840-000000000-00000.
2. Gurion, R., Vidal, L., Gafter-Gvili, A., Belnik, Y., Yeshurun, M., Raanani, P., and Shpilberg, O. (2010). 5-azacitidine prolongs overall survival in patients with myelodysplastic syndrome–a systematic review and meta-analysis. Haematologica *95*, 303–310. https://doi.org/10.3324/haematol.2009.010611.
3. Fenaux, P., Mufti, G.J., Hellstrom-Lindberg, E., Santini, V., Finelli, C., Giagounidis, A., Schoch, R., Gattermann, N., Sanz, G., List, A., et al. (2009). Efficacy of azacitidine compared with that of conventional care regimens in the treatment of higher-risk myelodysplastic syndromes: a randomised, open-label, phase III study. Lancet Oncol. *10*, 223–232. https://doi.org/10.1016/s1470-2045(09)70003-8.
4. Cazzola, M. (2020). Myelodysplastic Syndromes. N. Engl. J. Med. *383*, 1358–1374. https://doi.org/10.1056/NEJMra1904794.
5. Helbig, G., Chromik, K., Woźniczka, K., Kopińska, A.J., Boral, K., Dworaczek, M., Koclęga, A., Armatys, A., Panz-Klapuch, M., and Markiewicz, M. (2019). Real Life Data on Efficacy and Safety of Azacitidine Therapy for Myelodysplastic Syndrome, Chronic Myelomonocytic Leukemia and Acute Myeloid Leukemia. Pathol. Oncol. Res. *25*, 1175–1180. https://doi.org/10.1007/s12253-018-00574-0.
6. Rajakumaraswamy, N., Gandhi, M., Wei, A.H., Sallman, D.A., Daver, N.G., Mo, S., Iqbal, S., Karalliyadda, R., Chen, M., Wang, Y., and Vyas, P. (2024). Real-world Effectiveness of Azacitidine in Treatment-Naive Patients With Higher-risk Myelodysplastic Syndromes. Clin. Lymphoma Myeloma Leuk. *24*, 260–268.e2. https://doi.org/10.1016/j.clml.2023.12.008.
7. Prébet, T., Gore, S.D., Thépot, S., Esterni, B., Quesnel, B., Beyne Rauzy, O., Dreyfus, F., Gardin, C., Fenaux, P., and Vey, N. (2012). Outcome of acute myeloid leukaemia following myelodysplastic syndrome after azacitidine treatment failure. Br. J. Haematol. *157*, 764–766. https://doi.org/10.1111/j.1365-2141.2012.09076.x.

8. Zeidan, A.M., Stahl, M., DeVeaux, M., Giri, S., Huntington, S., Podoltsev, N., Wang, R., Ma, X., Davidoff, A.J., and Gore, S.D. (2018). Counseling patients with higher-risk MDS regarding survival with azacitidine therapy: are we using realistic estimates? Blood Cancer J. *8*, 55. https://doi.org/10.1038/s41408-018-0081-8.

9. Itzykson, R., Kosmider, O., Cluzeau, T., Mansat-De Mas, V., Dreyfus, F., Beyne-Rauzy, O., Quesnel, B., Vey, N., Gelsi-Boyer, V., Raynaud, S., et al. (2011). Impact of TET2 mutations on response rate to azacitidine in myelodysplastic syndromes and low blast count acute myeloid leukemias. Leukemia *25*, 1147–1152. https://doi.org/10.1038/leu.2011.71.

10. Bejar, R., Lord, A., Stevenson, K., Bar-Natan, M., Pérez-Ladaga, A., Zaneveld, J., Wang, H., Caughey, B., Stojanov, P., Getz, G., et al. (2014). TET2 mutations predict response to hypomethylating agents in myelodysplastic syndrome patients. Blood *124*, 2705–2712. https://doi.org/10.1182/blood-2014-06-582809.

11. Follo, M.Y., Pellagatti, A., Armstrong, R.N., Ratti, S., Mongiorgi, S., De Fanti, S., Bochicchio, M.T., Russo, D., Gobbi, M., Miglino, M., et al. (2019). Response of high-risk MDS to azacitidine and lenalidomide is impacted by baseline and acquired mutations in a cluster of three inositide-specific genes. Leukemia *33*, 2276–2290. https://doi.org/10.1038/s41375-019-0416-x.

12. Kim, K., Park, S., Choi, H., Kim, H.J., Kwon, Y.R., Ryu, D., Kim, M., Kim, T. M., and Kim, Y.J. (2020). Gene expression signatures associated with sensitivity to azacitidine in myelodysplastic syndromes. Sci. Rep. *10*, 19555. https://doi.org/10.1038/s41598-020-76510-7.

13. Cabezón, M., Malinverni, R., Bargay, J., Xicoy, B., Marcé, S., Garrido, A., Tormo, M., Arenillas, L., Coll, R., Borras, J., et al. (2021). Different methylation signatures at diagnosis in patients with high-risk myelodysplastic syndromes and secondary acute myeloid leukemia predict azacitidine response and longer survival. Clin. Epigenetics *13*, 9. https://doi.org/10.1186/s13148-021-01002-y.

14. Voso, M.T., Santini, V., Fabiani, E., Fianchi, L., Criscuolo, M., Falconi, G., Guidi, F., Hohaus, S., and Leone, G. (2014). Why methylation is not a marker predictive of response to hypomethylating agents. Haematologica *99*, 613–619. https://doi.org/10.3324/haematol.2013.099549.

15. Lee, E.J., and Zeidan, A.M. (2015). Genome sequencing in myelodysplastic syndromes: can molecular mutations predict benefit from hypomethylating agent therapy? Expert Rev. Hematol. *8*, 155–158. https://doi.org/10.1586/17474086.2015.1016905.

16. Nazha, A., Sekeres, M.A., Gore, S.D., and Zeidan, A.M. (2015). Molecular Testing in Myelodysplastic Syndromes for the Practicing Oncologist: Will the Progress Fulfill the Promise? Oncologist *20*, 1069–1076. https://doi.org/10.1634/theoncologist.2015-0067.

17. Kuendgen, A., Müller-Thomas, C., Lauseker, M., Haferlach, T., Urbaniak, P., Schroeder, T., Brings, C., Wulfert, M., Meggendorfer, M., Hildebrandt, B., et al. (2018). Efficacy of azacitidine is independent of molecular and clinical characteristics - an analysis of 128 patients with myelodysplastic syndromes or acute myeloid leukemia and a review of the literature. Oncotarget *9*, 27882–27894. https://doi.org/10.18632/oncotarget.25328.

18. Thurman, R.E., Rynes, E., Humbert, R., Vierstra, J., Maurano, M.T., Haugen, E., Sheffield, N.C., Stergachis, A.B., Wang, H., Vernot, B., et al. (2012). The accessible chromatin landscape of the human genome. Nature *489*, 75–82. https://doi.org/10.1038/nature11232.

19. Buenrostro, J.D., Giresi, P.G., Zaba, L.C., Chang, H.Y., and Greenleaf, W. J. (2013). Transposition of native chromatin for fast and sensitive epigenomic profiling of open chromatin, DNA-binding proteins and nucleosome position. Nat. Methods *10*, 1213–1218. https://doi.org/10.1038/nmeth.2688.

20. Corces, M.R., Buenrostro, J.D., Wu, B., Greenside, P.G., Chan, S.M., Koenig, J.L., Snyder, M.P., Pritchard, J.K., Kundaje, A., Greenleaf, W.J., et al. (2016). Lineage-specific and single-cell chromatin accessibility charts human hematopoiesis and leukemia evolution. Nat. Genet. *48*, 1193–1203. https://doi.org/10.1038/ng.3646.

21. Ma, S., Zhang, B., LaFave, L.M., Earl, A.S., Chiang, Z., Hu, Y., Ding, J., Brack, A., Kartha, V.K., Tay, T., et al. (2020). Chromatin Potential Identified by Shared Single-Cell Profiling of RNA and Chromatin. Cell *183*, 1103–1116.e20. https://doi.org/10.1016/j.cell.2020.09.056.

22. Ranzoni, A.M., Tangherloni, A., Berest, I., Riva, S.G., Myers, B., Strzelecka, P.M., Xu, J., Panada, E., Mohorianu, I., Zaugg, J.B., and Cvejic, A. (2021). Integrative Single-Cell RNA-Seq and ATAC-Seq Analysis of Human Developmental Hematopoiesis. Cell Stem Cell *28*, 472–487.e7. https://doi.org/10.1016/j.stem.2020.11.015.

23. Nerlov, C., and Graf, T. (1998). PU.1 induces myeloid lineage commitment in multipotent hematopoietic progenitors. Genes Dev. *12*, 2403–2412. https://doi.org/10.1101/gad.12.15.2403.

24. McIvor, Z., Hein, S., Fiegler, H., Schroeder, T., Stocking, C., Just, U., and Cross, M. (2003). Transient expression of PU.1 commits multipotent progenitors to a myeloid fate whereas continued expression favors macrophage over granulocyte differentiation. Exp. Hematol. *31*, 39–47. https://doi.org/10.1016/s0301-472x(02)01017-2.

25. Anderson, M.K., Weiss, A.H., Hernandez-Hoyos, G., Dionne, C.J., and Rothenberg, E.V. (2002). Constitutive expression of PU.1 in fetal hematopoietic progenitors blocks T cell development at the pro-T cell stage. Immunity *16*, 285–296. https://doi.org/10.1016/s1074-7613(02)00277-7.

26. Rothenberg, E.V., Hosokawa, H., and Ungerbäck, J. (2019). Mechanisms of Action of Hematopoietic Transcription Factor PU.1 in Initiation of T-Cell Development. Front. Immunol. *10*, 228. https://doi.org/10.3389/fimmu.2019.00228.

27. Meng, Y.S., Khoury, H., Dick, J.E., and Minden, M.D. (2005). Oncogenic potential of the transcription factor LYL1 in acute myeloblastic leukemia. Leukemia *19*, 1941–1947. https://doi.org/10.1038/sj.leu.2403836.

28. Subramanian, S., Thoms, J.A.I., Huang, Y., Cornejo-Páramo, P., Koch, F. C., Jacquelin, S., Shen, S., Song, E., Joshi, S., Brownlee, C., et al. (2023). Genome-wide transcription factor-binding maps reveal cell-specific changes in the regulatory architecture of human HSPCs. Blood *142*, 1448–1462. https://doi.org/10.1182/blood.2023021120.

29. Glavey, S.V., Manier, S., Natoni, A., Sacco, A., Moschetta, M., Reagan, M. R., Murillo, L.S., Sahin, I., Wu, P., Mishima, Y., et al. (2014). The sialyltransferase ST3GAL6 influences homing and survival in multiple myeloma. Blood *124*, 1765–1776. https://doi.org/10.1182/blood-2014-03-560862.

30. Sood, R., Kamikubo, Y., and Liu, P. (2017). Role of RUNX1 in hematological malignancies. Blood *129*, 2070–2082. https://doi.org/10.1182/blood-2016-10-687830.

31. Thoms, J.A.I., Koch, F.C., Raei, A., Subramanian, S., Wong, J.W.H., Vafaee, F., and Pimanda, J.E. (2024). BloodChIP Xtra: an expanded database of comparative genome-wide transcription factor binding and gene-expression profiles in healthy human stem/progenitor subsets and leukemic cells. Nucleic Acids Res. *52*, D1131–D1137. https://doi.org/10.1093/nar/gkad918.

32. Miraglia, S., Godfrey, W., Yin, A.H., Atkins, K., Warnke, R., Holden, J.T., Bray, R.A., Waller, E.K., and Buck, D.W. (1997). A novel five-transmembrane hematopoietic stem cell antigen: isolation, characterization, and molecular cloning. Blood *90*, 5013–5021.

33. Godfrey, L., Crump, N.T., O'Byrne, S., Lau, I.J., Rice, S., Harman, J.R., Jackson, T., Elliott, N., Buck, G., Connor, C., et al. (2021). H3K79me2/3 controls enhancer–promoter interactions and activation of the pan-cancer stem cell marker PROM1/CD133 in MLL-AF4 leukemia cells. Leukemia *35*, 90–106. https://doi.org/10.1038/s41375-020-0808-y.

34. Unnikrishnan, A., Papaemmanuil, E., Beck, D., Deshpande, N.P., Verma, A., Kumari, A., Woll, P.S., Richards, L.A., Knezevic, K., Chandrakanthan, V., et al. (2017). Integrative Genomics Identifies the Molecular Basis of Resistance to Azacitidine Therapy in Myelodysplastic Syndromes. Cell Rep. *20*, 572–585. https://doi.org/10.1016/j.celrep.2017.06.067.

35. Intlekofer, A.M., Takemoto, N., Wherry, E.J., Longworth, S.A., Northrup, J. T., Palanivel, V.R., Mullen, A.C., Gasink, C.R., Kaech, S.M., Miller, J.D., et al. (2005). Effector and memory CD8+ T cell fate coupled by T-bet

and eomesodermin. Nat. Immunol. *6*, 1236–1244. https://doi.org/10.1038/ni1268.

36. Llaó-Cid, L., Roessner, P.M., Chapaprieta, V., Öztürk, S., Roider, T., Bordas, M., Izcue, A., Colomer, D., Dietrich, S., Stilgenbauer, S., et al. (2021). EOMES is essential for antitumor activity of CD8(+) T cells in chronic lymphocytic leukemia. Leukemia *35*, 3152–3162. https://doi.org/10.1038/s41375-021-01198-1.
37. Newman, A.M., Steen, C.B., Liu, C.L., Gentles, A.J., Chaudhuri, A.A., Scherer, F., Khodadoust, M.S., Esfahani, M.S., Luca, B.A., Steiner, D., et al. (2019). Determining cell type abundance and expression from bulk tissues with digital cytometry. Nat. Biotechnol. *37*, 773–782. https://doi.org/10.1038/s41587-019-0114-2.
38. Szklarczyk, D., Gable, A.L., Lyon, D., Junge, A., Wyder, S., Huerta-Cepas, J., Simonovic, M., Doncheva, N.T., Morris, J.H., Bork, P., et al. (2019). STRING v11: protein-protein association networks with increased coverage, supporting functional discovery in genome-wide experimental datasets. Nucleic Acids Res. *47*, D607–D613. https://doi.org/10.1093/nar/gky1131.
39. Giles, J.R., Manne, S., Freilich, E., Oldridge, D.A., Baxter, A.E., George, S., Chen, Z., Huang, H., Chilukuri, L., Carberry, M., et al. (2022). Human epigenetic and transcriptional T cell differentiation atlas for identifying functional T cell-specific enhancers. Immunity *55*, 557–574.e7. https://doi.org/10.1016/j.immuni.2022.02.004.
40. Yang, H., Bueso-Ramos, C., DiNardo, C., Estecio, M.R., Davanlou, M., Geng, Q.R., Fang, Z., Nguyen, M., Pierce, S., Wei, Y., et al. (2014). Expression of PD-L1, PD-L2, PD-1 and CTLA4 in myelodysplastic syndromes is enhanced by treatment with hypomethylating agents. Leukemia *28*, 1280–1288. https://doi.org/10.1038/leu.2013.355.
41. Rodriguez-Sevilla, J.J., and Colla, S. (2024). T-cell dysfunctions in myelodysplastic syndromes. Blood *143*, 1329–1343. https://doi.org/10.1182/blood.2023023166.
42. Vierstra, J., Lazar, J., Sandstrom, R., Halow, J., Lee, K., Bates, D., Diegel, M., Dunn, D., Neri, F., Haugen, E., et al. (2020). Global reference mapping of human transcription factor footprints. Nature *583*, 729–736. https://doi.org/10.1038/s41586-020-2528-x.
43. Voskoboinik, I., Whisstock, J.C., and Trapani, J.A. (2015). Perforin and granzymes: function, dysfunction and human pathology. Nat. Rev. Immunol. *15*, 388–400. https://doi.org/10.1038/nri3839.
44. Vemulawada, C., Renavikar, P.S., Crawford, M.P., Steward-Tharp, S., and Karandikar, N.J. (2024). Disruption of IFNγ, GZMB, PRF1, or LYST Results in Reduced Suppressive Function in Human CD8+ T Cells. J. Immunol. *212*, 1722–1732. https://doi.org/10.4049/jimmunol.2300388.
45. Araki, Y., Fann, M., Wersto, R., and Weng, N.P. (2008). Histone acetylation facilitates rapid and robust memory CD8 T cell response through differential expression of effector molecules (eomesodermin and its targets: perforin and granzyme B). J. Immunol. *180*, 8102–8108. https://doi.org/10.4049/jimmunol.180.12.8102.
46. Tasis, A., Papaioannou, N.E., Grigoriou, M., Paschalidis, N., Loukogiannaki, C., Filia, A., Katsiki, K., Lamprianidou, E., Papadopoulos, V., Rimpa, C.M., et al. (2024). Single-Cell Analysis of Bone Marrow CD8+ T Cells in Myeloid Neoplasms Reveals Pathways Associated with Disease Progression and Response to Treatment with Azacitidine. Cancer Res. Commun. *4*, 3067–3083. https://doi.org/10.1158/2767-9764.Crc-24-0310.
47. Chiappinelli, K.B., Strissel, P.L., Desrichard, A., Li, H., Henke, C., Akman, B., Hein, A., Rote, N.S., Cope, L.M., Snyder, A., et al. (2015). Inhibiting DNA Methylation Causes an Interferon Response in Cancer via dsRNA Including Endogenous Retroviruses. Cell *162*, 974–986. https://doi.org/10.1016/j.cell.2015.07.011.
48. Roulois, D., Loo Yau, H., Singhania, R., Wang, Y., Danesh, A., Shen, S.Y., Han, H., Liang, G., Jones, P.A., Pugh, T.J., et al. (2015). DNA-Demethylating Agents Target Colorectal Cancer Cells by Inducing Viral Mimicry by Endogenous Transcripts. Cell *162*, 961–973. https://doi.org/10.1016/j.cell.2015.07.056.
49. Loo Yau, H., Bell, E., Ettayebi, I., de Almeida, F.C., Boukhaled, G.M., Shen, S.Y., Allard, D., Morancho, B., Marhon, S.A., Ishak, C.A., et al. (2021). DNA hypomethylating agents increase activation and cytolytic activity of CD8 (+) T cells. Mol. Cell *81*, 1469–1483.e8. https://doi.org/10.1016/j.molcel.2021.01.038.
50. Gang, A.O., Frøsig, T.M., Brimnes, M.K., Lyngaa, R., Treppendahl, M.B., Grønbæk, K., Dufva, I.H., Straten, P.T., and Hadrup, S.R. (2014). 5-Azacytidine treatment sensitizes tumor cells to T-cell mediated cytotoxicity and modulates NK cells in patients with myeloid malignancies. Blood Cancer J. *4*, e197. https://doi.org/10.1038/bcj.2014.14.
51. Stone, M.L., Chiappinelli, K.B., Li, H., Murphy, L.M., Travers, M.E., Topper, M.J., Mathios, D., Lim, M., Shih, I.M., Wang, T.L., et al. (2017). Epigenetic therapy activates type I interferon signaling in murine ovarian cancer to reduce immunosuppression and tumor burden. Proc. Natl. Acad. Sci. USA *114*, E10981–E10990. https://doi.org/10.1073/pnas.1712514114.
52. Ebelt, N.D., Zuniga, E., Johnson, B.L., Diamond, D.J., and Manuel, E.R. (2020). 5-Azacytidine Potentiates Anti-tumor Immunity in a Model of Pancreatic Ductal Adenocarcinoma. Front. Immunol. *11*, 538. https://doi.org/10.3389/fimmu.2020.00538.
53. Ohtani, H., Ørskov, A.D., Helbo, A.S., Gillberg, L., Liu, M., Zhou, W., Ungerstedt, J., Hellström-Lindberg, E., Sun, W., Liang, G., et al. (2020). Activation of a Subset of Evolutionarily Young Transposable Elements and Innate Immunity Are Linked to Clinical Responses to 5-Azacytidine. Cancer Res. *80*, 2441–2450. https://doi.org/10.1158/0008-5472.Can-19-1696.
54. Thoms, J.A.I., Yan, F., Hampton, H.R., Davidson, S., Joshi, S., Saw, J., Sarowar, C.H., Lim, X.Y., Nunez, A.C., Kakadia, P.M., et al. (2025). Clinical response to azacitidine in MDS is associated with distinct DNA methylation changes in HSPCs. Nat. Commun. *16*, 4451. https://doi.org/10.1038/s41467-025-59796-x.
55. Langmead, B., and Salzberg, S.L. (2012). Fast gapped-read alignment with Bowtie 2. Nat. Methods *9*, 357–359. https://doi.org/10.1038/nmeth.1923.
56. Zhang, Y., Liu, T., Meyer, C.A., Eeckhoute, J., Johnson, D.S., Bernstein, B.E., Nusbaum, C., Myers, R.M., Brown, M., Li, W., and Liu, X.S. (2008). Model-based Analysis of ChIP-Seq (MACS). Genome Biol. *9*, R137. https://doi.org/10.1186/gb-2008-9-9-r137.
57. Hinrichs, A.S., Karolchik, D., Baertsch, R., Barber, G.P., Bejerano, G., Clawson, H., Diekhans, M., Furey, T.S., Harte, R.A., Hsu, F., et al. (2006). The UCSC Genome Browser Database: update 2006. Nucleic Acids Res. *34*, D590–D598. https://doi.org/10.1093/nar/gkj144.
58. Arber, D.A., Orazi, A., Hasserjian, R., Thiele, J., Borowitz, M.J., Le Beau, M.M., Bloomfield, C.D., Cazzola, M., and Vardiman, J.W. (2016). The 2016 revision to the World Health Organization classification of myeloid neoplasms and acute leukemia. Blood *127*, 2391–2405.
59. Cheson, B.D., Greenberg, P.L., Bennett, J.M., Lowenberg, B., Wijermans, P.W., Nimer, S.D., Pinto, A., Beran, M., De Witte, T.M., Stone, R.M., and Mittelman, M. (2006). Clinical application and proposal for modification of the International Working Group (IWG) response criteria in myelodysplasia. Blood *108*, 419–425.
60. Corces, M.R., Trevino, A.E., Hamilton, E.G., Greenside, P.G., Sinnott-Armstrong, N.A., Vesuna, S., Satpathy, A.T., Rubin, A.J., Montine, K.S., Wu, B., et al. (2017). An improved ATAC-seq protocol reduces background and enables interrogation of frozen tissues. Nat. Methods *14*, 959–962. https://doi.org/10.1038/nmeth.4396.
61. Corces, M.R., Granja, J.M., Shams, S., Louie, B.H., Seoane, J.A., Zhou, W., Silva, T.C., Groeneveld, C., Wong, C.K., Cho, S.W., et al. (2018). The chromatin accessibility landscape of primary human cancers. Science *362*, eaav1898. https://doi.org/10.1126/science.aav1898.

STAR★METHODS

KEY RESOURCES TABLE

REAGENT or RESOURCE	SOURCE	IDENTIFIER
Antibodies		
Mouse anti-CD4-FITC	BD Biosciences	Cat#555346; RRID:AB_395751
Mouse anti-CD8-PerCP-Cy5.5-A	BD Biosciences	Cat#341050; RRID:AB_2811219
Mouse anti-CD34-PE	BD Biosciences	Cat#555822; RRID:AB_396151
Mouse anti-CD45-APC	BD Biosciences	Cat#555485; RRID:AB_398600
Biological samples		
Bone marrow samples from HR-MDS patients	Seoul St. Mary's Hematology Hospital	IRB: KC18TESE0700, KC16TISI0438
Healthy bone marrow controls	Seoul St. Mary's Hematology Hospital	IRB: KC18TESE0700, KC16TISI0438
Primary AML patient samples	Seoul St. Mary's Hematology Hospital	IRB: KC18TESE0700, KC16TISI0438
Chemicals, peptides, and recombinant proteins		
CTL Anti-Aggregate wash solution	CTL	Cat#CTL-AA-010
Ficoll-Paque plus	Cytiva	Cat#GE17-1440-02
Critical commercial assays		
CD4 MicroBeads, human	Miltenyi Biotec	Cat#130-097-048
CD8 MicroBeads, human	Miltenyi Biotec	Cat#130-045-201
Annexin V MicroBead Kit	Miltenyi Biotec	Cat#130-090-201
Deposited data		
Processed ATAC-seq data	This paper	GEO: GSE291718
Software and algorithms		
Bowtie2 version 2.5.3	Langmead and Salzberg[55]	http://bowtie-bio.sourceforge.net/bowtie2/
MACS2 version 2.2.9.1	Zhang et al.[56]	https://pypi.org/project/MACS2/
CIBERSORTx	Newman et al.[37]	https://cibersortx.stanford.edu
liftOver	Hinrichs et al.[57]	https://genome.ucsc.edu/cgi-bin/hgLiftOver

EXPERIMENTAL MODEL AND STUDY PARTICIPANT DETAILS

Patient information: Sample acquisition and clinical course

Pre-AZA treatment bone marrow aspirates were obtained from a total of 23 adult MDS patients who went on to receive AZA at Seoul St. Mary's Hospital between December 2009 and June 2021. As the study was planned in 2020, the classification of MDS and the response assessment for AZA were set to follow the 2016 WHO Classification[58] and the 2006 IWG Response Criteria,[59] respectively. As outlined in Table 1, the patients were classified as follows: RCMD (*n* = 1), MDS-EB1 (*n* = 6), and MDS-EB2 (*n* = 16). Of these, 15 patients were assessed as AZA responders, while 8 patients were assessed as non-responders. The non-responder group consisted of seven cases showing primary resistance, with progression to AML (*n* = 5) or MDS-EB2 (*n* = 2), and 1 case with stable disease without any hematological improvement (SD-HI) after four cycles of AZA, who then proceeded to HCT. Additionally, 13 AML patients were used to compare the chromatin accessibility profiles between primary AML and MDS samples (Table S1). The patient-derived MDS and AML samples were collected in a prospective cohort study with IRB approval from Seoul St. Mary's Hematology Hospital (KC18TESE0700, KC16TISI0438). ATAC-seq and data analysis were also approved by the IRBs of Ulsan National Institute of Science and Technology (Approval No. UNISTIRB-20-16-C). All patients provided informed consent, and the study adhered to the Declaration of Helsinki.

METHOD DETAILS

Sample preparation and cell isolation

Bone marrow mononuclear cells were isolated by Ficoll-Paque Plus density gradient centrifugation and cryopreserved without further fractionation. For analysis, cells were thawed in a 37°C water bath, washed twice with pre-warmed CTL Anti-Aggregate wash solution at 37°C, followed by one wash with phosphate-buffered saline at room temperature. Apoptotic cells were removed using Annexin-V magnetic beads according to manufacturer's instructions.

Flow cytometry and cell sorting

The distributions of cells stained with anti-CD4-FITC, anti-CD8-PerCP-Cy5.5-A and anti-CD34-PE were assessed in the anti-CD45-APC positive population among viable bone marrow cells. Positive selection of $CD4^+$ and $CD8^+$ T cells was performed using CD4 and CD8 microbeads according to the manufacturer's instructions. The percentage of $CD4^+$ and $CD8^+$ T cells in the selected cells was analyzed using the BD FACS LSR Fortessa (BD Biosciences), with CD4 and CD8 monoclonal antibodies. Using sorted $CD4^+$ and $CD8^+$ T cells, ATAC-seq libraries were prepared. For all samples, quality control was performed based on TSS scores and only high-quality data was selected (TSS >3.0, hg38 Refseq), ultimately yielding ATAC-seq data from 10 bone marrow samples: three healthy controls (HC), four MDS non-responders (MDS-NR), and three MDS responders (MDS-R).

ATAC-seq library preparation

Bulk ATAC-seq was performed using 50,000 cells per sample following the Omni-ATAC-seq protocol.[60] Briefly, cells were permeabilized and tagmented using in-house produced Tn5[61] transposase at 37°C for 30 minutes. Libraries were amplified using barcoded primers. All libraries were sequenced using paired-end sequencing on Illumina NovaSeq 6000 or NovaSeq X platforms.

Processing bulk ATAC-seq data for analysis

ATAC-seq data processing was done as previously described.[61] Briefly, we mapped the reads to the human reference genome (hg38) using Bowtie2 (v 2.5.3). The reads that mapped with low quality (MAPQ <10), that were not properly paired in mapping, or mapped to chrM and blacklist regions were discarded. Peak summits called using MACS2 (v 2.2.9.1) were extended 250 bp to each end, followed by iterative overlap peak merging as described previously.[61]

Unsupervised k-means clustering and cluster purity

Cluster purity was determined as described previously.[20] Samples were clustered in two clusters using k-means clustering with all features from ATAC-seq, DNA methylation sequencing,[13] or RNA-seq,[12] respectively. The cluster was assigned to the most featured one; for example, if more than half of the samples were responders, the sample cluster was assigned to the responder group. The counts of correctly assigned samples were used to measure the cluster purity, which indicates the accuracy of clustering.

Identification of AZA-response-related ATAC peaks

The distal binarization approach[61] was employed to identify 1,940 AZA-response-related ATAC peaks. First, a fold change threshold of 1.5 was applied to determine peaks specific to AZA responders and non-responders. Peaks with a p-value below 0.05 were considered statistically significant. This analysis led to the identification of 1,940 AZA-response-related ATAC peaks, consisting of 733 non-responder-specific peaks and 1,207 responder-specific peaks. To further validate the significance of the group-specific peaks, the permutation test was performed. The group labels were randomly shuffled, ensuring that at least half of the labels were altered. The distal binarization method was then applied to the shuffled data to select differential peaks. By comparing the results obtained from the permuted data with the original 1,940 peaks, the identified peaks were shown not to be the result of random events.

TF motif enrichment analysis

Non-redundant transcription factor motifs[42] were used to find TF motifs enriched in peak clusters. The archetype MEME models (v 2.0) were first converted to position weight matrix format to allow processing by motifmatchr (v 1.28.0). Using all motifs as a background, the p-value of the hypergeometric test was used to determine the enrichment of each TF.

Cell composition analysis using CIBERSORTx

To calculate the composition of human hematopoietic cell types in bone marrow samples, we used CIBERSORTx. The signature matrix is publicly available[20] but had to be first converted to hg38 using liftOver. Using the peak regions annotated by the signature matrix, the Tn5 insertion frequency was scored for each MDS sample, and the count was normalized by quartile normalization. The signature matrix and the count matrix were then used for CIBERSORTx as performed with 1,000 permutations.

Comparison with $CD8^+$ T cell subsets

Data from human $CD8^+$ T cell subsets were obtained from the Gene Expression Omnibus database, accession number GSE179613. The data were curated based on the following criteria: samples from individuals with ATAC-seq data for all $CD8^+$ T cell subsets, individual samples from the same laboratory to minimize batch effects, and inclusion of more than three individuals in each batch set. This selection process ensured data consistency and minimized potential technical variations. After applying these criteria, four donors that perfectly fitted our requirements were identified and were included in our analysis.

QUANTIFICATION AND STATISTICAL ANALYSIS

Statistical analyses were performed using R version 4.0 or later. Statistical significance for group comparisons was assessed using Wilcoxon rank-sum tests. For flow cytometry validation, correlation analysis between CIBERSORTx predictions and experimental measurements was performed using Pearson correlation (n = 8 samples). Statistical significance for group comparisons was assessed using Wilcoxon rank-sum tests for non-parametric data. All statistical tests were two-sided, and p-values <0.05 were considered statistically significant. The exact value of n, statistical tests used, and significance thresholds are reported in individual figure legends.